AGU PUBLICATIONS

Geophysical Research Letters

RESEARCH LETTER
10.1002/2016GL068146

Key Points:
- Impact of irrigation extents over several thousand kilometers
- Two responsible mechanisms are advective water vapor transport and shifts in supraregional patterns
- Decline/increase in irrigation will likely result in reduction/increase in precipitation in remote regions

Supporting Information:
- Supporting Information S1

Correspondence to:
P. de Vrese,
philipp.de-vrese@mpimet.mpg.de

Citation:
de Vrese, P., S. Hagemann, and M. Claussen (2016), Asian irrigation, African rain: Remote impacts of irrigation, *Geophys. Res. Lett.*, *43*, 3737–3745, doi:10.1002/2016GL068146.

Received 5 FEB 2016
Accepted 3 MAR 2016
Accepted article online 9 MAR 2016
Published online 20 APR 2016

Asian irrigation, African rain: Remote impacts of irrigation

Philipp de Vrese[1], Stefan Hagemann[1], and Martin Claussen[1,2]

[1]Max Planck Institute for Meteorology, Hamburg, Germany, [2]Center for Earth System Research and Sustainability, University of Hamburg, Hamburg, Germany

Abstract Irrigation is not only vital for global food security but also constitutes an anthropogenic land use change, known to have strong effects on local hydrological and energy cycles. Using the Max Planck Institute for Meteorology's Earth System Model, we show that related impacts are not confined regionally but that possibly as much as 40% of the present-day precipitation in some of the arid regions in Eastern Africa are related to irrigation-based agriculture in Asia. Irrigation in South Asia also substantially influences the climate throughout Southeast Asia and China via the advection of water vapor and by altering the Asian monsoon. The simulated impact of irrigation on remote regions is sensitive to the magnitude of the irrigation-induced moisture flux. Therefore, it is likely that a future extension or decline of irrigated areas due to increasing food demand or declining fresh water resources will also affect precipitation and temperatures in remote regions.

1. Introduction

Irrigation-based agriculture plays an essential role for global food security and for the welfare of a large share of the world's population, as it provides about 40% of the global crop production [*Siebert et al.*, 2005]. Furthermore, it has a substantial impact on global water resources, and currently about 70% of humanity's demand for fresh water originate from irrigation [*Wada et al.*, 2013]. With a growing world population, these numbers are expected to increase rather than decrease in the foreseeable future [*De Fraiture and Wichelns*, 2010]. Irrigation-based agriculture is not only affected by changing climate conditions and declining fresh water resources, but in turn has a substantial effect on them. It strongly influences the hydrological cycle and the land surface energy budget by the redistribution of water. Currently, irrigation-induced evapotranspiration is estimated to be as high as 2600 $km^3\ a^{-1}$ which corresponds to about 4% of the total terrestrial evapotranspiration [*Gordon et al.*, 2005; *Oki and Kanae*, 2006].

The influence of irrigation on local climate has been the focus of numerous investigations. Especially with respect to South Asia, a profound impact on regional circulations such as the Indian monsoon, precipitation, and surface temperatures has been established in model-based regional studies [*Adegoke et al.*, 2003; *Douglas et al.*, 2006; *Kueppers et al.*, 2007; *Douglas et al.*, 2009; *Lobell et al.*, 2009; *Saeed et al.*, 2009; *Lee et al.*, 2009; *Niyogi et al.*, 2010; *Lucas-Picher et al.*, 2011; *Harding et al.*, 2013; *Lo and Famiglietti*, 2013; *Huber et al.*, 2014; *Tuinenburg et al.*, 2014; *Alter et al.*, 2015]. The sheer amount of water introduced into the atmosphere suggests that irrigation also has a distinct influence on global climate, but only few studies exist which investigate the impact of irrigation on this scale [*Boucher et al.*, 2004; *Lobell et al.*, 2006; *Sacks et al.*, 2009; *Puma and Cook*, 2010; *Cook et al.*, 2011, 2014]. These studies identified the general mechanisms by which irrigation affects the state of the land surface and the atmosphere and provides rough estimates of its aggregate impact on global climate. At the surface, irrigation leads to an evaporative cooling, while within the atmosphere the additional water vapor may results in an increased absorption of solar radiation and an amplification of the greenhouse effect which is intensified by a condensational heat release [*Boucher et al.*, 2004]. Furthermore, changes in water vapor and temperature profiles affect essential atmospheric processes such as convection, cloud formation, and precipitation [*Sacks et al.*, 2009]. However, the existing global scale studies have not explored in depth the dynamic mechanisms by which irrigation in certain regions translates to an impact on the state of the surface and the atmosphere in regions a substantial distance from the irrigated areas.

Focusing on irrigation in Asia, we aim to quantify the impact of irrigation in remote regions (in distances $\sim 10^3$ km) and to identify the mechanisms responsible. For this investigation on an intercontinental and transcontinental scale we analyzed simulations performed with the Max Planck Institute for Meteorology's

general circulation model ECHAM6 [*Stevens et al.*, 2013] coupled to the land surface model JSBACH [*Brovkin et al.*, 2009], into which a simple irrigation scheme was implemented.

2. Methods

All simulations cover the years 1979–1999. From these, the first year was required for the spin-up of the model and is not considered in the analysis. In the simulations sea-surface temperature and sea-ice extent were prescribed, according to the protocol of the Atmospheric Model Intercomparison Project (AMIP) [*Gates et al.*, 1999]. The model was run using a temporal resolution of 20 min and a vertical resolution of 47 model levels, of which the lowest is located on a height of about 30 m. The horizontal resolution of the simulations was T63, which corresponds to a grid spacing of about 200 km in tropical latitudes. The grid boxes located on land are further subdivided into homogeneous grid box subareas, the so called tiles. The cover fraction of the irrigated crop tile was derived from the fifth version of the global map of irrigation areas [*Siebert et al.*, 2005, 2013]. For more details on the model see supporting information Text S1.

For the simulations, JSBACH was equipped with an irrigation scheme in which the soil moisture in the irrigated fraction of the land surface was artificially maintained at a certain level [*Tuinenburg et al.*, 2014]. This best resembles irrigation via a flooding of the surface as there is no interception by the canopy layer. In this approach, the amount of irrigation is determined by the state of saturation of the soil and the vegetation cover rather than by management techniques and the availability of water. For example, for India the highest demand for irrigation is simulated for the end of the Rabi season (December–March) and for the perennial crops during April and May, whereas there is only little demand during the Kharif season (June–October) and the beginning of the Rabi season (November–December) because of the high soil moisture content resulting from the monsoon rains.

To account for uncertainties due to simplifications required for the representation of irrigation, two simulations were performed that differ strongly in their impact on the net vertical moisture flux. For the first simulation (IRR_{min}), irrigation is calculated in a way that maintains the soil moisture close to the level at which plants make optimal use of the available water but that does not lead to evaporation from nonvegetated areas and the skin reservoir.

Rice growing regions constitute about 43% of the global irrigation water demand and most of the rice is produced on fully inundated paddy fields [*Bouman et al.*, 2007]. As in these regions the soils are actually saturated for the largest part of the growing season, evaporation from the nonvegetated parts of the fields may have a strong contribution to the overall moisture flux, especially at the beginning of the growing season when a field is not fully covered by vegetation. Consequently, the above scheme likely underestimates the net moisture flux from irrigation. Thus, we designed a second scenario in which irrigation is simulated in a way that also induces evaporation from nonvegetated parts of the agricultural areas (IRR_{max}). For this scenario, the soil moisture in irrigated regions was maintained at the field capacity, to best represent inundated surfaces in rice growing regions, and we prescribed a certain fraction of the nonvegetated part of the grid box to be irrigated.

Additionally, an idealized irrigation simulation (IRR_{ideal}) was performed to investigate the distance between irrigated regions and areas in which impacts due to irrigation are still perceivable. Here irrigation was modeled analogous to IRR_{max} but with irrigation limited to a region in Asia between 0°N–45°N and 30°E–95°E from which also the Arabian Peninsula was excluded. For more details on the irrigation scheme see supporting information Text S2.

To estimate the impact of simulated irrigation on the state of the surface and atmosphere and the surface energy and moisture fluxes, the above irrigation simulations were compared to a reference simulation REF. This simulation is identical to IRR_{min} but without a representation of irrigation in the respective areas.

To determine whether differences between two simulations constitute a robust impact at the grid box level, their statistical significance was calculated with a two-sample, two-sided student's t test ($p < 0.05$). When comparing the results of individual simulations, the t test is not necessarily a conclusive measure. The most common strategy to mitigate the test's weaknesses is to evaluate differences between ensembles, ideally with a large number of ensemble members, i.e., $n > 10$. However, to avoid the large computational costs of such ensemble simulations, a strategy was used, similar to the one applied by *Hagemann et al.* [2009], in which the differences between simulations are evaluated against the ensemble spread as a measure of the model's

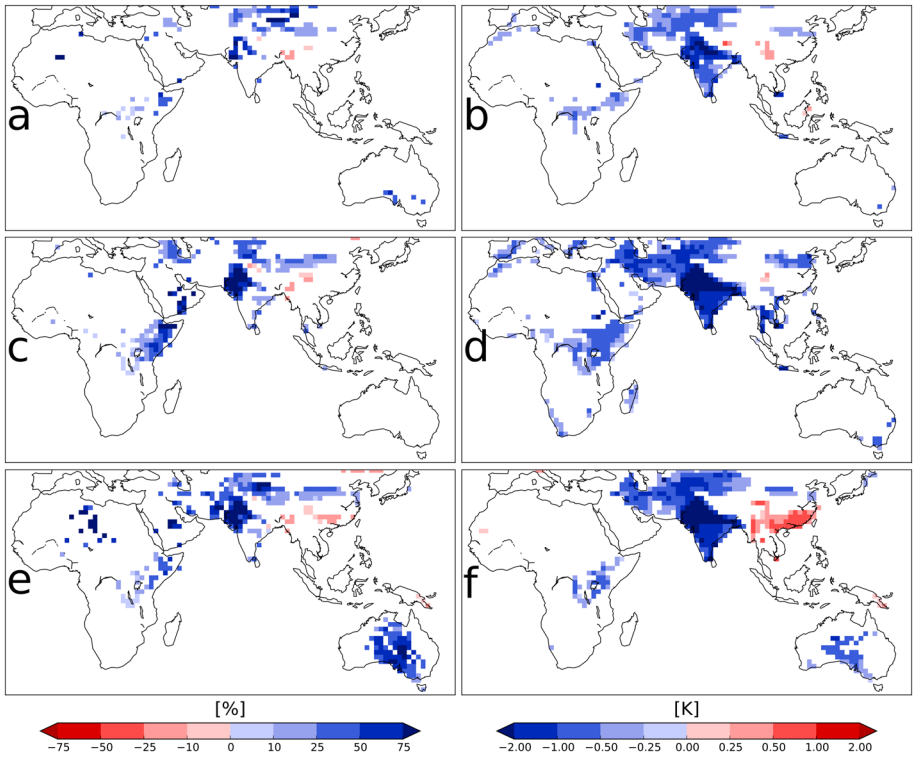

Figure 1. Impact of irrigation on precipitation and land surface temperature: relative difference in 20 year annual mean precipitation over land (a) (IRR_{min} − REF) / REF, (c) (IRR_{max} − REF)/ REF, and (e) (IRR_{ideal} − REF)/ REF; 20 year annual mean land surface temperature difference (b) IRR_{min} − REF, (d) IRR_{max} − REF, and (f) IRR_{ideal} − REF; nonrobust impacts are masked in white.

internal variability. Here we combine both measures, *t* test and internal variability, and differences at the grid box level are considered to be robust if they are statistically significant and above ECHAM/JSBACH's internal variability. The latter was derived from three five-member ensembles of 20 year AMIP-style simulations. For more details on the internal variability see supporting information Text S3.

3. Impact of Irrigation on Remote Regions

With respect to the scenario IRR_{min}, irrigation-based agriculture has a robust impact on the simulated near-surface climate in between 5% and 15% of the global land surface (depending on the variable considered), even though irrigated agricultural land covers only about 2%. Most of the affected areas are located in heavily irrigated regions such as South Asia (Figure 1). However, there are also regions such as Eastern Africa which contain only a small share of irrigated areas themselves but which exhibit pronounced impacts. In the following, we will show how the advective moisture transport and changes in regional circulations lead to substantial impacts in these remote regions. Note that here the term advection is also used as a synonym for a sequence of consecutive advection, precipitation, and reevaporation.

Figure 2a schematically shows the relevant winds in the lower troposphere (up to about 4 km) during boreal spring and summer for the region around the northern Indian Ocean (simulated in IRR_{min}; for more information on the simulated winds and how they compare to reanalysis data see supporting information Figure 1). At the onset of boreal spring (February–March) the evaporative moisture flux from irrigation in South Asia is already pronounced and the amount of water applied during irrigation is well above 20 mm mo^{-1} (supporting information Figure 2). Due to the resulting increase in evapotranspiration, the low-level atmospheric specific humidity in the respective region is up to 0.5 g kg^{-1} larger in IRR_{min} than in REF (Figure 2b). At this time, the low-level winds in the Arabian Sea are in southwesterly direction. Consequently, a large fraction of the atmospheric water vapor, originating from irrigation in South Asia, is advected across the Arabian Sea toward Africa's east coast, where the specific humidity increases distinctly (by up to 0.7 g kg^{-1}). During this period, the upward moisture flux (evapotranspiration-precipitation) along the main wind

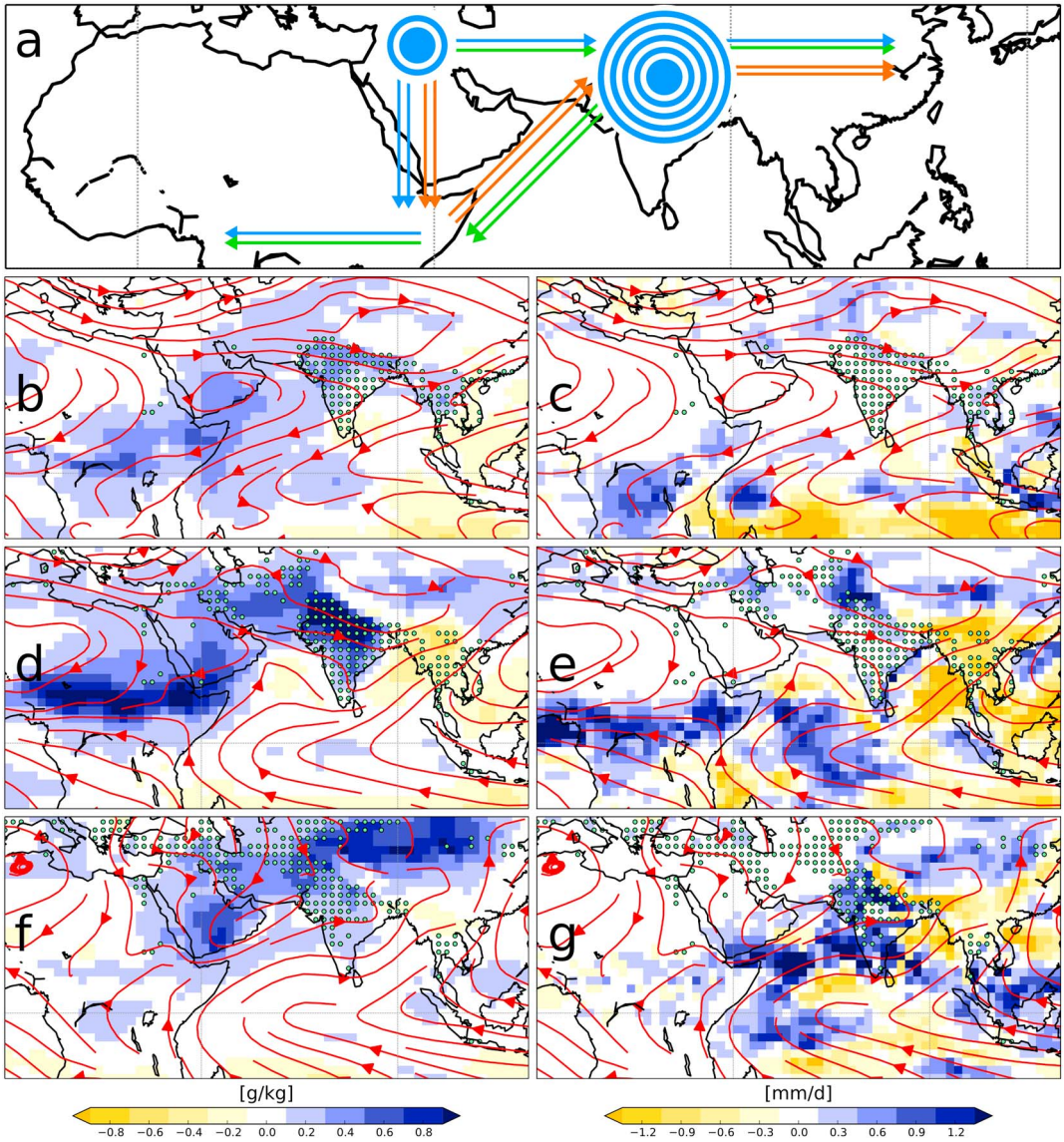

Figure 2. Advection of water vapor: (a) Schematic of low-level tropospheric winds during early spring (green arrows), late spring (blue arrows), and summer (orange arrows) from irrigated regions (blue circles); 20 year mean difference in specific humidity (IRR_{min} − REF) in the low atmosphere (1000 − 600 hpa): (b) February–March, (d) April–May, and (f) June–July; precipitation difference (IRR_{min} − REF): (c) February–March, (e) April–May, and (g) June–July; red streamlines indicate the direction of low-level tropospheric winds (1000 − 600 hpa) in the irrigation simulation, dotted areas indicate grid box mean irrigation >3 mm month^{-1}.

direction in the Arabian sea is negative (see supporting information Figure 3), and the additional water vapor in the atmosphere does not originate from evaporation over the Indian Ocean.

Between April and May the winds in the Arabian Sea turn so that the moisture advection from South Asia toward Africa ceases (Figure 2d). At this time, irrigation in the Middle East, Turkmenistan, and Afghanistan increases notably. Water vapor stemming from evapotranspiration in this region is transported toward the Horn of Africa, where the northerly winds are diverted westward by southeasterly dryer winds. This transport leads to an increase in specific humidity of more than 1.0 g kg^{-1} at Africa's east coast but also in regions as far west as Nigeria.

During summer (June–July) the wind field over Africa changes and the northerly winds carrying water vapor from irrigated regions are diverted eastward across the Arabian Sea (Figure 2f). Accordingly, there is still a pronounced humidity transport into the Arabian Peninsula and the region around the Horn of Africa

but the subsequent westward water vapor transport ceases. With winds turning north-eastward over the Arabian Sea, the atmospheric water vapor is advected toward China rather than Africa (Figure 2f). Consequently, the increase in specific humidity in some regions in China becomes exceedingly pronounced, i.e., by up to 1.0 g kg^{-1}. Note that the additional atmospheric water vapor from irrigation in eastern China and Southeast Asia is predominantly transported eastward over the Pacific.

Depending on the local saturation vapor pressure, the increase in atmospheric water vapor can lead to a distinct increase in precipitation. During spring, the additionally advected water vapor results in an increase in precipitation in Africa of up to 1.0 mm d^{-1} (Figures 2c and 2e). The same is true for the water vapor advected across China during late spring and summer (Figures 2e and 2g). With the onset of the summer monsoon around June, precipitation increases and less irrigation is simulated in IRR_{min} (supporting information Figure S2). Therefore, starting in August the differences in specific humidity between the IRR_{min} and REF decrease (not shown).

The effects of the advective transport described above are partly increased by changes in the wind field and by increasing upward moisture fluxes over certain regions in the Indian Ocean. For example, in April and May, the easterly winds at the Gulf of Guinea are weaker in IRR_{min} which reduces the offshore water vapor transport and enhances the moisture convergence over Africa (see supporting information Figure S3).

Even though these processes are limited to boreal spring and summer, irrigation notably impacts the annual mean climate in remote regions (see supporting information Figure S4). As shown above, water vapor is transported to regions in a substantial distance downwind of the irrigated areas, where it leads to an annual mean precipitation increase of up to 0.5 mm d^{-1}. In some of the dryer areas in Eastern Africa, the increase in precipitation corresponds to more than a third of the annual mean precipitation (Figure 1). The increase in precipitation leads to increased evapotranspiration and an associated latent cooling of the surface. Furthermore, the additional atmospheric water vapor affects cloud formation, i.e., annual mean aggregate cloud cover in the lower troposphere increases in parts by more than 7.5%, which reduces incoming solar radiation at the surface. In combination, these two effects induce a cooling of the surface in remote regions of up to 0.5 K.

The increase in upward moisture flux for IRR_{max} (2453 km^3 a^{-1}) is more than twice as pronounced as for IRR_{min} (1019 km^3 a^{-1}). Both scenarios fall within the range of estimates from previous studies. IRR_{max} is close to the upper limit of estimates and it is likely that the present irrigation-induced moisture flux is closer to the one simulated in IRR_{min} [*Gordon et al.*, 2005; *Wada et al.*, 2013; *Yoshikawa et al.*, 2013]. Nonetheless, it can be seen that the remote impacts are sensitive to the magnitude of the moisture flux related to irrigation. Consequently, the two simulations show the same general mechanisms by which irrigation affects remote regions, but the magnitude of the impact on climate differs strongly between them (see supporting information Figure S5). For example, with respect to IRR_{min}, the robust increase in annual mean precipitation in Eastern and Central Africa can be as high as 40% but is below 25% within the majority of the grid boxes. For IRR_{max}, on the other hand, the area that exhibits relative increases of more than 25% almost entirely covers eastern Ethiopia, Kenya, and parts of Somalia (Figure 1). Even when limiting the simulated irrigation in IRR_{max} to a region in Asia between 0°N–45°N and 30°E–95°E, from which also the Arabian Peninsula was excluded (IRR_{ideal}), the increase in atmospheric water vapor and precipitation in Africa is still larger than for IRR_{min}. This confirms that the major impact on precipitation in Eastern Africa is attributable to irrigation occurring outside of Africa.

Irrigation also has a direct effect on regional atmospheric circulations and associated precipitation patterns such as the South and East Asian monsoon. The evaporative cooling in irrigated areas, especially in India causes a weakening of the summer monsoon by altering the land sea thermal contrast that drives the monsoon winds [*Douglas et al.*, 2009; *Lucas-Picher et al.*, 2011]. Accordingly, the associated onshore winds during May and August are weaker in IRR_{min} than in REF (Figure 3).

In heavily irrigated regions, a reduction of monsoon precipitation is masked by an increase in evapotranspiration from irrigated areas and an enhanced local moisture recycling. However, in regions with a smaller extent of irrigated areas, a precipitation decrease limits the available water at the surface, which leads to decreased evapotranspiration and higher surface temperatures. This effect can be seen, e.g., in Southeast Asia and southern China, where between May and July precipitation is reduced by up to 2.0 mm d^{-1} and surface temperature increases by up to 1.0 K (Figure 3, supporting information Figure S2). These findings are corroborated

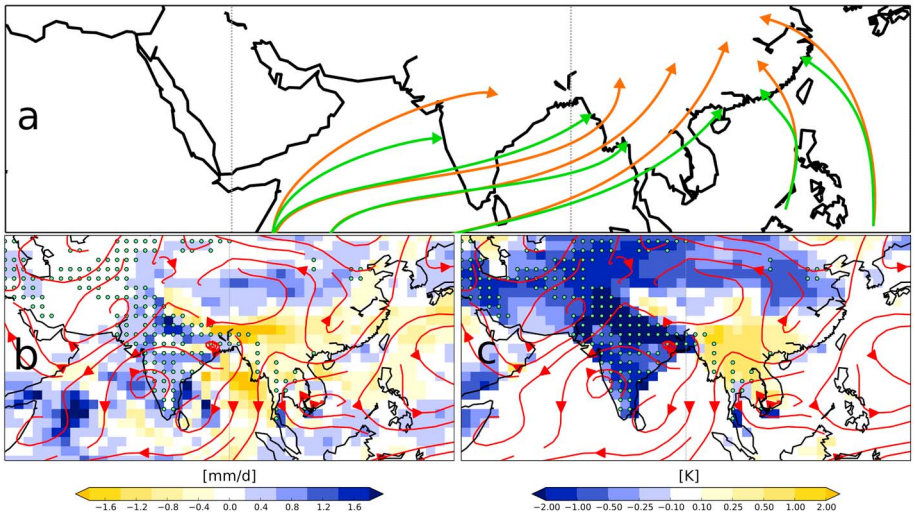

Figure 3. Impact on Asian monsoon: (a) Schematic of winds related to the Asian summer monsoon, with (green arrows) and without (orange arrows) irrigation-induced surface cooling; 20 year mean May-July difference (IRR_{min} − REF): (b) precipitation and (c) surface temperature; red streamlines indicate differences (IRR_{min} − REF) in the direction of the low-level winds (1000 − 600 hpa), dotted areas indicate grid box mean irrigation >3 mm $month^{-1}$.

by modeling studies, using higher resolved regional models, that showed irrigation to cause a reduction of the onshore winds in South Asia, leading to a decrease in precipitation in regions in India, Bangladesh, Nepal, and Myanmar [*Saeed et al.*, 2009; *Tuinenburg et al.*, 2014]. However, due to the limited domain size, these studies could not show the extensive spatial scale of these impacts.

4. Conclusion and Discussions

We identified the advection of water vapor and alterations of the Asian monsoon as key mechanisms by which irrigation in the Middle East and South Asia directly impacts the climate in distances of several thousand kilometers. The strength of the simulated impact of irrigation on remote regions is sensitive to the magnitude of the irrigation-induced moisture flux, which has important implications with respect to real world irrigation. It may be inferred that as a consequence of a possible decline in irrigated areas in the Middle East or in South Asia, precipitation would likely decrease in remote regions. Some regions in India are already threatened by a possible local ground water depletion in the not-too-distant future [*Puma and Cook*, 2010; *Elliott et al.*, 2013]. This is especially relevant for vulnerable regions in Eastern Africa, where droughts frequently cause humanitarian catastrophes that affect millions of people [*Maxwell and Fitzpatrick*, 2012]. In the respective regions, up to 40% of the simulated annual mean precipitation can be a related to irrigation on the Asian continent.

Given the importance of these effects, it is the key to reduce the respective uncertainties. As is the case for any model-based study, the findings of this investigation are sensitive to the formulations incorporated in the model. The sensitivity of irrigation-induced climate effects to changes in certain structural aspects of ECHAM6 and JSBACH is being investigated as part of an ongoing study. The results presented here have been selected from a range of simulations, because they were performed with the most physically accurate parametrizations and showed the best agreement with observational data, i.e., WATCH Forcing Data [*Weedon et al.*, 2011].

Furthermore, global simulations performed with other models exhibit remote impacts that are comparable in magnitude to those presented in this study. For example, *Lobell et al.* [2009] find a surface cooling of more than 1 K (seasonally averaged) for large regions in northern, eastern, and even western Africa, even though they prescribed only a small fraction of irrigated areas in these regions. *Boucher et al.* [2004] find a surface cooling of up to 0.5 K in nonirrigated regions in Africa, and *Puma and Cook* [2010] and *Cook et al.* [2011] find a significant cooling of the surface and seasonally averaged increases in precipitation of up to 1 mm d^{-1}. Additionally, reanalysis data support the existence of remote impacts. *Wei et al.* [2013] find an increase in precipitation in Africa roughly between 0°N–20°N that is directly related to evapotranspiration in irrigated areas. In their study, a moisture tracking algorithm is used to estimate the share of precipitation that originates from

irrigation in Egypt. The study shows that from the relative precipitation increase of up to 5% in certain parts of Eastern Africa, less than 0.5% can be traced back to Egypt. As also the extent of local irrigation is comparatively small, this indicates that a major share of this precipitation increase is related to irrigation outside of Africa.

Despite this evidence, more studies are required that focus on the remote effects and the underlying mechanisms. On one hand these should include additional modeling studies, which account for feedbacks from the ocean. As we did not consider an interactive ocean in this study, the remote impacts may be modulated by ocean-atmosphere interactions, e.g., using an ocean model, *Cook et al.* [2014] found a stronger cooling of the land surface than the existing global studies that prescribed sea-surface temperature and sea-ice extent. Additionally, these studies could make use of moisture tracking schemes, as has been done for the regional scale [*Wei et al.*, 2013; *Tuinenburg et al.*, 2014].

On the other hand an effort needs to be made to study the remote impacts using observational and reanalysis data sets. The later is a challenging task, as it is impossible to directly determine the irrigation-related fraction of an observed variable, e.g., precipitation or atmospheric water vapor. Furthermore, there are large uncertainties in the observations [*Fekete et al.*, 2004] and also known issues with respect to reanalysis data [*Bengtsson et al.*, 2004]. An attempt made in this study to detect an impact of irrigation on the observed precipitation trend in Eastern Africa was inconclusive (see Appendix A).

Finally, we limited our investigations to the remote impacts in Eastern Africa, Southeast Asia, and southern China because here the underlying mechanisms are most clearly visible. However, the simulations performed in this study indicate that remote effects can also be found in other regions. Water vapor from irrigated areas is advected into Russia where it influences the near-surface climate, irrigation in southern Europe may have a strong effect on the atmospheric moisture content and surface temperatures in western Europe and Scandinavia and the idealized simulation indicated impacts on the near-surface climate in Australia. Even with significant advances in irrigation efficiency, the amount of water used for irrigation will likely increase by almost 50% (relative to 2000) until the year 2050 [*De Fraiture and Wichelns*, 2010; *Schneider et al.*, 2011], as irrigation-based agriculture has to meet the food and energy demand of a growing world population. Thus, certain aspects of future climate change are likely to be related to the remote effects of irrigation.

Appendix A: Observed Precipitation Trend in Africa

The fraction of irrigation-induced precipitation cannot be distinguished in observational data sets directly. Nonetheless, observed trends may provide indications for an impact on precipitation. *Siebert et al.* [2015] estimated that the extent of irrigated areas almost tripled during the second half of the twentieth century and the related moisture transport may have a noticeable effect on the precipitation trend in Eastern Africa for this period.

In fact, some observations (e.g., CRU [*Harris et al.*, 2013] and GPCC VASClimo [*Beck et al.*, 2005]) show increasing rainfall in parts of Eastern Africa between 1951 and 2000, while in the majority of Africa precipitation exhibits a negative trend. For the Horn of Africa, observations indicate an increase in precipitation also during boreal spring (Figure A1a), which is the time when the moisture transport from irrigated areas in Asia is most active. However, even though it is interesting that the Horn is the only larger region in Sub-Saharan Africa that exhibits an increase in precipitation, these trends are not statistically significant. Additionally, several studies suggest that precipitation trends in Eastern Africa are strongly influenced by changes in the sea-surface temperature in the Indian Ocean [*Behera et al.*, 2005; *Shongwe et al.*, 2011; *Yang et al.*, 2014; *Williams and Funk*, 2011; *Lyon and DeWitt*, 2012]. Thus, the observed precipitation trends do not disprove the existence of remote impacts of irrigation, but they also do not provide conclusive evidence for their importance.

To compare the observed trends to our model, two 52 year AMIP-style simulations, IRR_{50} and REF_{50}, were performed for the years 1949–2000. In the irrigation simulation the cover fraction of the irrigated crop tile was linearly increased between the years 1949 and 2000 (the cover fraction was assumed to triple during this period) and the soil moisture in the respective tile was maintained at the field capacity.

As the observations, neither of the simulations exhibited a statistically significant increase in precipitation for the second half of the last century. This confirms that the precipitation trend in Eastern Africa is strongly influenced by other processes than irrigation. However, the simulated precipitation is consistently closer to the observations when irrigation is accounted for in the model. This is especially true for the period between the 1950s and the 1980s (Figures A1b and A1c). Here the simulated precipitation is not only improved in the

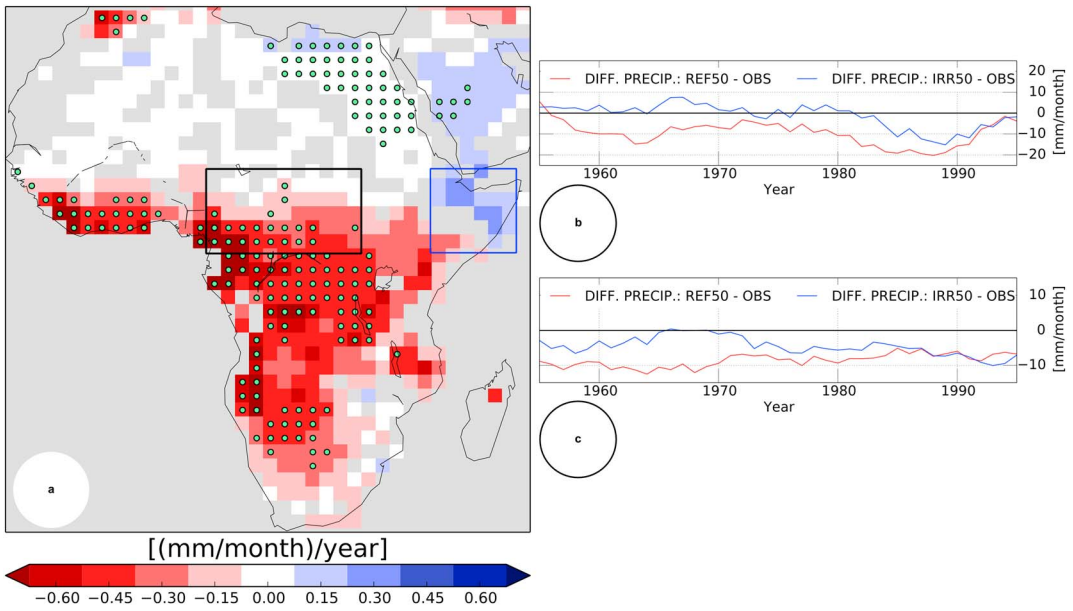

Figure A1. Precipitation trend in Africa: (a) March–May 1951–2000 precipitation trend (average of CRU [*Harris et al.*, 2013] and GPCC VASClimO data [*Beck et al.*, 2005]); dotted areas exhibit a statistically significant monotonic trend (Mann-Kendall test; $p < 0.05$); areas where data sets do not agree on the trend have been masked in grey. (b) Difference between simulated and observed March–May 1951–2000 precipitation at the Horn of Africa (39.4°–48.8°E and 4.7°–14.0°N, blue square in Figure A1a. The red line shows the 10 year running mean precipitation difference between the simulation without irrigation (REF_{50}) and observations, the blue line corresponds to the differences between the irrigation simulation (IRR_{50}) and observations. (c) Difference between simulated and observed March–May 1951–2000 precipitation east of the Gulf of Guinea (9.4°–28.8°E and 4.7°–14.0°N, black square in Figure A1a. The red line shows the 10 year running mean precipitation difference between the simulation without irrigation (REF_{50}) and observations, the blue line corresponds to the differences between the irrigation simulation (IRR_{50}) and observations.

region around the Horn of Africa (39.4°–48.8°E and 4.7° –14.0°N, Figure A1b) where the simulated impact of irrigation is most pronounced but also in regions east of the Gulf of Guinea (9.4°–28.8°E and 4.7°–14.0°N, Figure A1c), where observations indicate a strong reduction of precipitation. This indicates that there are several processes that govern the development of precipitation in Africa, one of which appears to be the extension of irrigated areas.

Acknowledgments
The authors declare that they have no competing financial interests. Data requests for materials should be addressed to philipp.de-vrese@mpimet.mpg.de.

References

Adegoke, J. O., R. A. Pielke, J. Eastman, R. Mahmood, and K. G. Hubbard (2003), Impact of irrigation on midsummer surface fluxes and temperature under dry synoptic conditions: A regional atmospheric model study of the U.S. high plains, *Mon. Weather Rev.*, *131*(3), 556–564.

Alter, R. E., Y. Fan, B. R. Lintner, and C. P. Weaver (2015), Observational evidence that Great Plains irrigation has enhanced summer precipitation intensity and totals in the midwestern United States, *J. Hydrometeorol.*, *16*(4), 1717–1735.

Beck, C., J. Grieser, B. Rudolf, and U. Schneider (2005), A new monthly precipitation climatology for the global land areas for the period 1951 to 2000, *Geophys. Res. Abstr.*, *7*, 181–190.

Behera, S. K., J.-J. Luo, S. Masson, P. Delecluse, S. Gualdi, A. Navarra, and T. Yamagata (2005), Paramount impact of the Indian Ocean dipole on the East African short rains: A CGCM study, *J. Clim.*, *18*(21), 4514–4530.

Bengtsson, L., S. Hagemann, and K. I. Hodges (2004), Can climate trends be calculated from reanalysis data?, *J. Geophys. Res.*, *109*, D11111, doi:10.1029/2004JD004536.

Boucher, O., G. Myhre, and A. Myhre (2004), Direct human influence of irrigation on atmospheric water vapour and climate, *Clim. Dyn.*, *22*(6–7), 597–603.

Bouman, B., R. Lampayan, and T. Tuong (2007), *Water Management in Irrigated Rice: Coping With Water Scarcity*, Int. Rice Res. Inst., Los Baños, Phil.

Brovkin, V., T. Raddatz, C. H. Reick, M. Claussen, and V. Gayler (2009), Global biogeophysical interactions between forest and climate, *Geophys. Res. Lett.*, *36*, L07405, doi:10.1029/2009GL037543.

Cook, B. I., M. J. Puma, and N. Y. Krakauer (2011), Irrigation induced surface cooling in the context of modern and increased greenhouse gas forcing, *Clim. Dyn.*, *37*(7–8), 1587–1600.

Cook, B. I., S. P. Shukla, M. J. Puma, and L. S. Nazarenko (2014), Irrigation as an historical climate forcing, *Clim. Dyn.*, *44*(5–6), 1715–1730.

De Fraiture, C., and D. Wichelns (2010), Satisfying future water demands for agriculture, *Agric. Water Manage.*, *97*(4), 502–511.

Douglas, E., D. Niyogi, S. Frolking, J. Yeluripati, R. A. Pielke, N. Niyogi, C. Vörösmarty, and U. Mohanty (2006), Changes in moisture and energy fluxes due to agricultural land use and irrigation in the indian monsoon belt, *Geophys. Res. Lett.*, *33*, L14403, doi:10.1029/2006GL026550.

Douglas, E., A. Beltrán-Przekurat, D. Niyogi, R. Pielke Sr, and C. Vörösmarty (2009), The impact of agricultural intensification and irrigation on land–atmosphere interactions and indian monsoon precipitation—A mesoscale modeling perspective, *Global Planet. Change*, *67*(1), 117–128.

Elliott, J., et al. (2013), Constraints and potentials of future irrigation water availability on agricultural production under climate change, *Proc. Natl. Acad. Sci. U.S.A.*, *111*(9), 3239–3244.

Fekete, B. M., C. J. Vörösmarty, J. O. Roads, and C. J. Willmott (2004), Uncertainties in precipitation and their impacts on runoff estimates, *J. Clim.*, *17*(2), 294–304.

Gates, W. L., et al. (1999), An overview of the results of the Atmospheric Model Intercomparison Project (AMIP 1), *Bull. Am. Meteorol. Soc.*, *80*(1), 29–55.

Gordon, L. J., W. Steffen, B. F. Jönsson, C. Folke, M. Falkenmark, and Å. Johannessen (2005), Human modification of global water vapor flows from the land surface, *Proc. Natl. Acad. Sci. U.S.A.*, *102*(21), 7612–7617.

Hagemann, S., H. Göttel, D. Jacob, P. Lorenz, and E. Roeckner (2009), Improved regional scale processes reflected in projected hydrological changes over large European catchments, *Clim. Dyn.*, *32*(6), 767–781.

Harding, R., E. Blyth, O. Tuinenburg, and A. Wiltshire (2013), Land atmosphere feedbacks and their role in the water resources of the Ganges basin, *Sci. Total Environ.*, *468-469*, S85–S92.

Harris, I., P. Jones, T. Osborn, and D. Lister (2013), Updated high-resolution grids of monthly climatic observations—The CRU TS3.10 Dataset, *Int. J. Climatol.*, *34*(3), 623–642.

Huber, D., D. Mechem, and N. Brunsell (2014), The effects of Great Plains irrigation on the surface energy balance, regional circulation, and precipitation, *Climate*, *2*(2), 103–128.

Kueppers, L. M., M. A. Snyder, and L. C. Sloan (2007), Irrigation cooling effect: Regional climate forcing by land-use change, *Geophys. Res. Lett.*, *34*, L03703, doi:10.1029/2006GL028679.

Lee, E., T. N. Chase, B. Rajagopalan, R. G. Barry, T. W. Biggs, and P. J. Lawrence (2009), Effects of irrigation and vegetation activity on early Indian summer monsoon variability, *Int. J. Climatol.*, *29*(4), 573–581.

Lo, M.-H., and J. S. Famiglietti (2013), Irrigation in California's Central Valley strengthens the southwestern U.S. water cycle, *Geophys. Res. Lett.*, *40*, 301–306, doi:10.1002/grl.50108.

Lobell, D., G. Bala, and P. Duffy (2006), Biogeophysical impacts of cropland management changes on climate, *Geophys. Res. Lett.*, *33*, L06708, doi:10.1029/2005GL025492.

Lobell, D., G. Bala, A. Mirin, T. Phillips, R. Maxwell, and D. Rotman (2009), Regional differences in the influence of irrigation on climate, *J. Clim.*, *22*(8), 2248–2255.

Lucas-Picher, P., J. H. Christensen, F. Saeed, P. Kumar, S. Asharaf, B. Ahrens, A. J. Wiltshire, D. Jacob, and S. Hagemann (2011), Can regional climate models represent the Indian monsoon?, *J. Hydrometeorol.*, *12*(5), 849–868.

Lyon, B., and D. G. DeWitt (2012), A recent and abrupt decline in the east African long rains, *Geophys. Res. Lett.*, *39*, L02702, doi:10.1029/2011GL050337.

Maxwell, D., and M. Fitzpatrick (2012), The 2011 Somalia famine: Context, causes, and complications, *Global Food Secur.*, *1*(1), 5–12.

Niyogi, D., C. Kishtawal, S. Tripathi, and R. S. Govindaraju (2010), Observational evidence that agricultural intensification and land use change may be reducing the Indian summer monsoon rainfall, *Water Resour. Res.*, *46*, W03533, doi:10.1029/2008WR007082.

Oki, T., and S. Kanae (2006), Global hydrological cycles and world water resources, *Science*, *313*(5790), 1068–1072.

Puma, M. J., and B. I. Cook (2010), Effects of irrigation on global climate during the 20th century, *J. Geophys. Res.*, *115*, D16120, doi:10.1029/2010JD014122.

Sacks, W. J., B. I. Cook, N. Buenning, S. Levis, and J. H. Helkowski (2009), Effects of global irrigation on the near-surface climate, *Clim. Dyn.*, *33*(2–3), 159–175.

Saeed, F., S. Hagemann, and D. Jacob (2009), Impact of irrigation on the South Asian summer monsoon, *Geophys. Res. Lett.*, *36*, L20711, doi:10.1029/2009GL040625.

Schneider, U. A., et al. (2011), Impacts of population growth, economic development, and technical change on global food production and consumption, *Agric. Syst.*, *104*(2), 204–215.

Shongwe, M. E., G. J. van Oldenborgh, B. van den Hurk, and M. van Aalst (2011), Projected changes in mean and extreme precipitation in Africa under global warming. Part II: East Africa, *J. Clim.*, *24*(14), 3718–3733.

Siebert, S., P. Döll, J. Hoogeveen, J.-M. Faures, K. Frenken, and S. Feick (2005), Development and validation of the global map of irrigation areas, *Hydrol. Earth Syst. Sci. Discuss.*, *2*(4), 1299–1327.

Siebert, S., V. Henrich, K. Frenken, and J. Burke (2013), *Global Map of Irrigation Areas Version 5*, Rheinische Friedrich-Wilhelms-University, Bonn, Germany / Food and Agriculture Organization of the United Nations, Rome, Italy.

Siebert, S., M. Kummu, M. Porkka, P. Döll, N. Ramankutty, and B. R. Scanlon (2015), A global data set of the extent of irrigated land from 1900 to 2005, *Hydrol. Earth Syst. Sci. Discuss.*, *19*(3), 1521–1545.

Stevens, B., et al. (2013), Atmospheric component of the MPI-M Earth System Model: ECHAM6, *J. Adv. Model. Earth Syst.*, *5*(2), 146–172.

Tuinenburg, O., R. Hutjes, T. Stacke, A. Wiltshire, and P. Lucas-Picher (2014), Effects of irrigation in India on the atmospheric water budget, *J. Hydrometeorol.*, *15*(3), 1028–1050.

Wada, Y., et al. (2013), Multimodel projections and uncertainties of irrigation water demand under climate change, *Geophys. Res. Lett.*, *40*, 4626–4632, doi:10.1002/grl.50686.

Weedon, G. P., S. Gomes, P. Viterbo, W. J. Shuttleworth, E. Blyth, H. Oesterle, J. C. Adam, N. Bellouin, O. Boucher, and M. Best (2011), Creation of the WATCH forcing data and its use to assess global and regional reference crop evaporation over land during the twentieth century, *J. Hydrometeorol.*, *12*(5), 823–848.

Wei, J., P. A. Dirmeyer, D. Wisser, M. G. Bosilovich, and D. M. Mocko (2013), Where does the irrigation water go? an estimate of the contribution of irrigation to precipitation using MERRA, *J. Hydrometeorol.*, *14*(1), 275–289.

Williams, A. P., and C. Funk (2011), A westward extension of the warm pool leads to a westward extension of the Walker circulation, drying eastern Africa, *Clim. Dyn.*, *37*(11–12), 2417–2435.

Yang, W., R. Seager, M. A. Cane, and B. Lyon (2014), The east African long rains in observations and models, *J. Clim.*, *27*(19), 7185–7202.

Yoshikawa, S., J. Cho, H. Yamada, N. Hanasaki, A. Khajuria, and S. Kanae (2013), An assessment of global net irrigation water requirements from various water supply sources to sustain irrigation: Rivers and reservoirs (1960–2000 and 2050), *Hydrol. Earth Syst. Sci. Discuss.*, *10*(1), 1251–1288.